

Theory of magnetism in $\text{La}_2\text{NiMnO}_6$

Prabuddha Sanyal¹

¹ IIT Roorkee, Roorkee 247667, India

The magnetism of ordered and disordered $\text{La}_2\text{NiMnO}_6$ is explained using a model involving double exchange and superexchange. The concept of majority spin hybridization in the large coupling limit is used to explain the ferromagnetism of $\text{La}_2\text{NiMnO}_6$ as compared to the ferrimagnetism of $\text{Sr}_2\text{FeMoO}_6$. The ferromagnetic insulating ground state in the ordered phase is explained. The essential role played by the Ni-Mn superexchange between the Ni e_g electron spins and the Mn t_{2g} core electron spins in realizing this ground state, is outlined. In presence of antisite disorder, the model system is found to exhibit a tendency of becoming a spin-glass at low temperatures, while it continues to retain a ferromagnetic transition at higher temperatures, similar to recent experimental observations [D. Choudhury *et al.*, Phys. Rev. Lett. **108**, 127201 (2012)]. This reentrant spin-glass or reentrant ferromagnetic behaviour is explained in terms of the competition of the ferromagnetic double exchange between the Ni e_g and the Mn e_g electrons, and the ferromagnetic Ni-Mn superexchange, with the antiferromagnetic antisite Mn-Mn superexchange.

PACS numbers: 75.47.Lx, 75.10.-b, 75.50.Dd

I. INTRODUCTION

The double perovskite (DP) $\text{La}_2\text{NiMnO}_6$ (LNMO), has generated a lot of interest for its magnetodielectric properties¹, making it a promising candidate for potential device applications². There have also been suggestions of topological phases³ for LNMO formed in LaNiO_3 - LaMnO_3 superlattices. The pure compound is deemed to be a ferromagnetic semiconductor^{1,4}, with a Curie temperature very close to room temperature ($T_c \approx 280\text{K}$). Recently, there has been reports of reentrant spin-glass behaviour in partially disordered LNMO at low temperatures, along with a disordered ferromagnetism at higher temperatures⁵. In this paper, a simple theoretical model for LNMO is proposed which can explain the ferromagnetic insulating behaviour of the ordered compound, as well as provide insight into the low temperature spin-glass behaviour observed in the disordered case. Since there is supposed to be significant contribution of the relative spin-orientation dependent asymmetric hopping between the transition metal sites to the dielectric constant, hence the colossal magnetodielectricity is closely related to the magnetism⁵. Hence an understanding of the magnetic and electronic properties of this material is essential to the understanding of the magnetodielectricity in this material.

II. THE MODEL HAMILTONIAN

In $\text{La}_2\text{NiMnO}_6$ the Nickel is in Ni^{2+} state ($t_{2g}^6 e_g^2$) and has two e_g electrons, while the Manganese is in Mn^{4+} state ($t_{2g}^3 e_g^0$) and has three t_{2g} electrons^{1,5,6}. As the t_{2g} electrons are more localized, and are parallel due to strong Hund coupling, they may be thought of as a core classical spin $S = 3/2$. Nickel has a filled t_{2g} shell, and net t_{2g} spin $S = 0$, hence this compound can be thought of as a manganite where half the sites do not have a core spin. When Nickel e_g electrons hop on to the va-

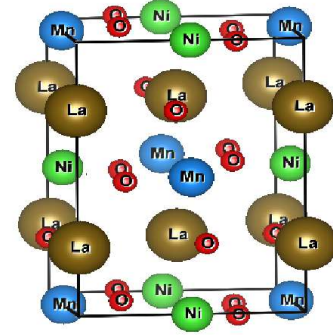


FIG. 1. (colour online) Crystal structure of $\text{La}_2\text{NiMnO}_6$

cant e_g orbitals of Manganese, they have an exchange with the large Mn t_{2g} core spins as usual, but the difference with most other DP-s like $\text{Sr}_2\text{FeMoO}_6$ (SFMO)⁷ and $\text{Sr}_2\text{CrOsO}_6$ (SCO)⁸ is that this exchange coupling is ferromagnetic rather than antiferromagnetic. A model with somewhat similar ingredients had been proposed in Ref⁹, but they only considered the ordered case numerically, and at zero temperature. A detailed understanding of the magnetism of LNMO including the case of antisite disorder is lacking so far. We propose the following simple model Hamiltonian for the ordered case:

$$\begin{aligned}
 H_{ord} = & \epsilon_{Ni} \sum_{i\sigma} c_{N,i\sigma}^\dagger c_{N,i\sigma} + \epsilon_{Mn} \sum_{i\sigma} c_{M,i\sigma}^\dagger c_{M,i\sigma} \\
 & + t_{MN} \sum_{\langle ij \rangle \sigma} c_{M,i\sigma}^\dagger c_{N,j\sigma} + J_H \sum_{i\alpha, \beta} c_{M,i\alpha}^\dagger \vec{\sigma}_{\alpha\beta} c_{M,i\beta} \cdot \vec{S}_i \\
 & + J_{super} \sum_{\langle ij \rangle} c_{N,j\alpha}^\dagger \vec{\sigma}_{\alpha\beta} c_{N,j\beta} \cdot \vec{S}_i \quad (1)
 \end{aligned}$$

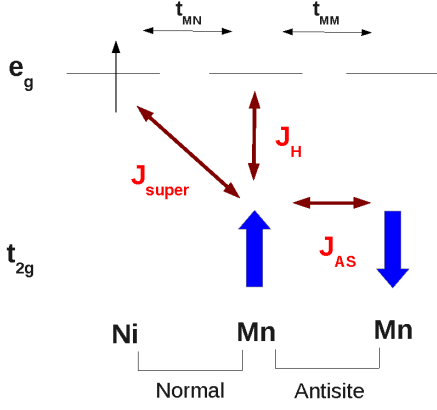


FIG. 2. (colour online) Exchange mechanisms for model Hamiltonian

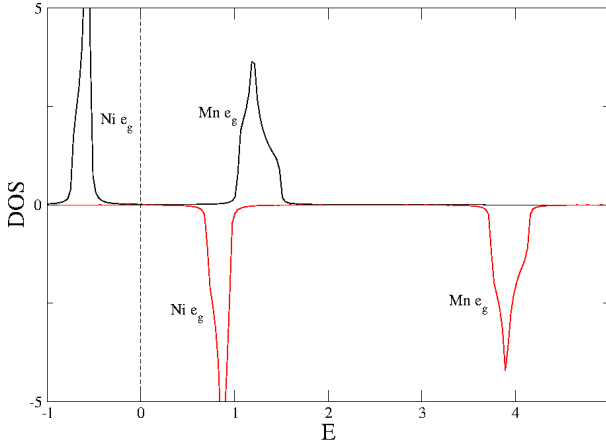


FIG. 3. (colour online) e_g electron DOS for ordered $\text{La}_2\text{NiMnO}_6$, from model Hamiltonian. Dotted line: Fermi energy.

where $c_{N,i\sigma}^\dagger$ ($c_{M,i\sigma}^\dagger$) creates an electron at the i -th Ni (Mn) site with spin σ . ϵ_{Ni} and ϵ_{Mn} are site energies of e_g electrons at the Ni and Mn sites respectively, while t_{MN} represents the hopping between the e_g orbitals of Ni and Mn. In our attempt to find the simplest Hamiltonian which can explain the magnetism of LNMO, we consider a single orbital model¹⁰. In addition to J_H which results in Ni-Mn $e_g - e_g$ double exchange, this Hamiltonian introduces for LNMO the Ni-Mn $e_g - t_{2g}$ superexchange J_{super} (see Fig 2), which will be found to set the scale of the ferromagnetic T_C , similar to the Cr-Os superexchange in SCO¹¹. Such a superexchange had earlier been calculated⁶ for LNMO in the context of Kugel-Khomskii model¹² and found to be ferromagnetic¹³. The parameter choice is phenomenological, but motivated from the DFT results of Ref⁶. It is to be noted that the Kondo coupling between the core and itinerant spin on the B site is ferromagnetic for LNMO (and is equal to the Hund coupling J_H), and not antiferromagnetic as in case of

SFMO^{7,14} (See Appendix). If one considers the limit of large coupling, $J_H \rightarrow -\infty$ ¹⁵⁻¹⁷, then this Hamiltonian simplifies further:

$$\begin{aligned}
 H_{ord}^{(1)} = & \epsilon_{Ni} \sum_{i\sigma} c_{N,i\sigma}^\dagger c_{N,i\sigma} + \tilde{\epsilon}_{Mn} \sum_i m_i^\dagger m_i \\
 & + t_{MN} \sum_{\langle ij \rangle} \left(\cos \frac{\theta_i}{2} m_i^\dagger c_{N,j\uparrow} + \sin \frac{\theta_i}{2} e^{i\phi_i} m_i^\dagger c_{N,j\downarrow} \right) \\
 & + J_{super} \sum_{\langle ij \rangle} c_{N,j\alpha}^\dagger \vec{\sigma}_{\alpha\beta} c_{N,j\beta} \cdot \vec{S}_i \quad (2)
 \end{aligned}$$

where m^\dagger represents spinless Mn degree of freedom, θ_i is the polar angle between the spin \vec{S}_i at i -th Mn site with z -axis, ϕ_i is the azimuthal angle, and charge transfer energy is given by $\Delta = \tilde{\epsilon}_{Mn} - \epsilon_{Ni}$. This represents the minimal model for understanding the magnetism of ordered LNMO. It is to be noted that this Hamiltonian has *majority spin hybridization* between Mn and Ni, i.e., in case of a fully ferromagnetic arrangement of the B-site (Mn) core spins ($\theta_i = 0$, $\phi_i = 0 \forall i$), *B-B' (Mn-Ni) hybridization in the DP $A_2BB'O_6$ ($\text{La}_2\text{NiMnO}_6$) is only possible in the majority spin channel, rather than in the minority spin channel as in DP-s like SFMO¹⁸ and SCO⁸* (See Appendix).

Antisite disordered regions (with B,B' interchanged) have strong antiferromagnetic superexchange between two nearest-neighbour B site ions, eg. half-filled Fe^{3+} ions in case of SFMO¹⁹, or half-filled Mn^{4+} ions in case of LNMO. Hence in the disordered case, the following terms are added¹⁸:

$$\begin{aligned}
 H_{disord} = & t_{MM} \sum_{\langle ij \rangle} \left[\cos \frac{\theta_i}{2} \cos \frac{\theta_j}{2} \right. \\
 & \left. + e^{i(\phi_j - \phi_i)} \sin \frac{\theta_i}{2} \sin \frac{\theta_j}{2} \right] m_i^\dagger m_j \\
 & + t_{NN} \sum_{\langle ij \rangle \sigma} c_{N,i\sigma}^\dagger c_{N,j\sigma} + J_{AS} \sum_{\langle ij \rangle} \vec{S}_i \cdot \vec{S}_j \quad (3)
 \end{aligned}$$

where J_{AS} is an antiferromagnetic superexchange in the antisite region between two neighbouring Mn t_{2g} core spins (see Fig 2), while t_{MM} and t_{NN} represent hopping between two neighbouring Mn and two neighbouring Ni e_g levels respectively.

III. ORDERED CASE: DISPERSION AND DOS

In the ordered case, in the limit $|J_H| \rightarrow \infty$, the dispersion can be obtained analytically from Eq 2 in the ferromagnetic phase. There are 3 e_g bands, given by

$$\begin{aligned}
 \epsilon_1 = & \epsilon_{Ni} - z \frac{J_{super} S}{2} \quad (4) \\
 \epsilon_{\pm} = & 0.5 \left[(\epsilon_{Mn} + \epsilon_{Ni}) + \frac{(J_H + z J_{super}) S}{2} \right. \\
 & \left. \pm \sqrt{\left\{ (\epsilon_{Mn} - \epsilon_{Ni}) + \frac{(J_H - z J_{super}) S}{2} \right\}^2 + 4\epsilon_k^2} \right] \quad (5)
 \end{aligned}$$

where $\epsilon_k = 2t_{MN}(\cos k_x + \cos k_y)^7$.

At half-filling of the Ni e_g orbital in this single orbital model in the ferromagnetic state with all the core spins \vec{S} pointing up, the Ni e_g band in only one spin channel (the majority spin channel) is fully filled, and so the Fermi energy lies in a gap. This gap can be estimated in the limit of Ni-Mn $e_g - e_g$ hopping $t_{MN} = 0$, when the bands shrink to levels. Then $\epsilon_1 \approx \epsilon_{Ni} - \frac{zJ_{super}S}{2}$, $\epsilon_+ \approx \epsilon_{Mn} + \frac{J_H S}{2}$, and $\epsilon_- \approx \epsilon_{Ni} + \frac{zJ_{super}S}{2}$. ϵ_1 and ϵ_- now represent the two spin-split Ni e_g down (minority) and up (majority) levels respectively, while ϵ_+ represents the energy of the up (majority) Mn e_g orbital. The down (minority) Mn e_g orbital is shifted out to ∞ due to the $J_H \rightarrow -\infty$ limit being taken. Hence the energy gap in the majority spin channel between the occupied Ni orbital given by ϵ_- and the unoccupied Mn orbital given by ϵ_+ is given by

$$\begin{aligned} E_g &\approx \epsilon_+ - \epsilon_- \\ &\approx \Delta - \frac{zJ_{super}S}{2} \end{aligned} \quad (6)$$

Hence the gap in the majority spin channel can be estimated as $\Delta - \frac{zJ_{super}S}{2}$. Thus, a necessary condition for the Ferro-Insulating state is $\Delta > \frac{zJ_{super}S}{2}$. If the Ni-Mn hopping is turned on, then this condition becomes more stringent:

$$\Delta - \frac{zJ_{super}S}{2} > 8t_{MN} \quad (7)$$

However, if there was no Ni-Mn superexchange, the two Ni e_g levels for up and down spins would have coincided, and the Ni e_g band being half-filled, the system would have been metallic. In presence of the Ni-Mn superexchange, the Ni e_g levels are spin-split. The condition for non-overlapping of the Ni e_g bands can be estimated as $\epsilon_1 - \epsilon_- > 0$, which gives $-zJ_{super}S > 0$. This along with the inequality 7 are the conditions for the realization of a Ferromagnetic Insulator (FI) ground state. Hence the Ni-Mn superexchange, introduced in a model for LNMO in Eq 1 and Eq 2, is an important and essential component for obtaining the ferromagnetic insulating ground state in the ordered case. Thus electron correlations are an essential criterion for the realization of the FI ground state in this model of LNMO.

In the case of finite J_H , there are 4 e_g bands. In Fig 3, the DOS is plotted for $J_H = -0.9eV^6$ by numerically solving the 4×4 eigenvalue problem from Eq 1 in the ferromagnetic ground state for each \vec{k} and using $\rho(E) = \frac{1}{N} \sum_k \delta(E - \epsilon_k)$. The t_{2g} bands for Mn and Ni do not appear in the DOS as the t_{2g} electrons for Mn⁴⁺ and Ni²⁺ have been considered to be classical core spins of S=3/2 and S=0 respectively. With the Mn core t_{2g} spin considered to be in up state at all sites, it is found that the minority (down) spin Ni e_g band and the majority (up) spin Mn e_g band lie in between the majority (up) spin Ni e_g and the minority (down) spin Mn e_g bands, as in the DFT DOS of Ref⁶. The Fermi energy lies in

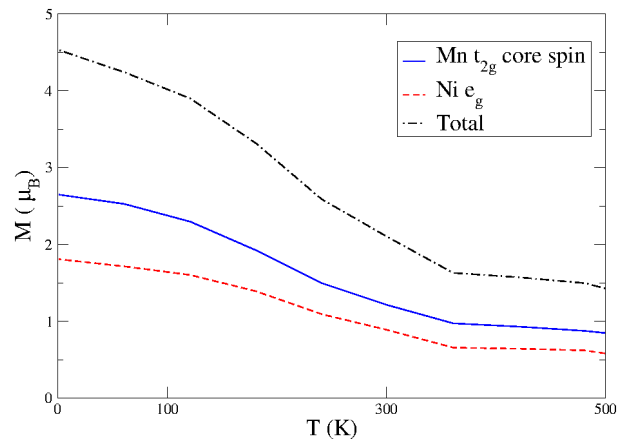


FIG. 4. (colour online) Mn t_{2g} core spin, Ni e_g electron spin and total moment as a function of temperature in the ordered case

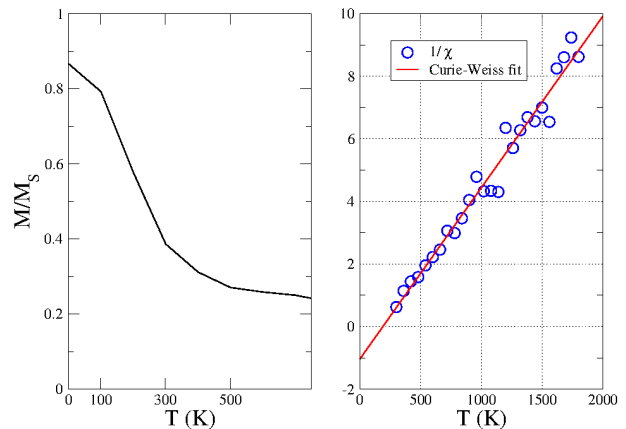


FIG. 5. (colour online) Left : $M-T$ plot for the ordered case in 2D. Right: Curie Weiss fit to the reciprocal susceptibility for the ordered case.

between the Ni e_g and the Mn e_g majority spin bands. Thus the ferromagnetic insulating state is explained. The separation between the Ni e_g and Mn e_g bands in the minority spin channel is almost twice that in the majority spin channel, once again similar to the DFT DOS. The band gap in the majority spin channel ($\approx 1eV$) is also reproduced. Thus the relative band positions are roughly similar to that of the published DFT results²⁰.

IV. ORDERED CASE: MAGNETISM

Exact Diagonalization-Monte Carlo (ED-MC) simulations were performed with the hamiltonian $H_{ord}^{(1)}$ given by Eq 2, and a system size of 8×8 in 2D, and $8 \times 8 \times 8$ in 3D. The moments at the Nickel site, Manganese site and the total moment are plotted in Fig 4. It is observed that the B and B' site moments are parallel to each other, rather than antiparallel as in Sr₂FeMoO₆.

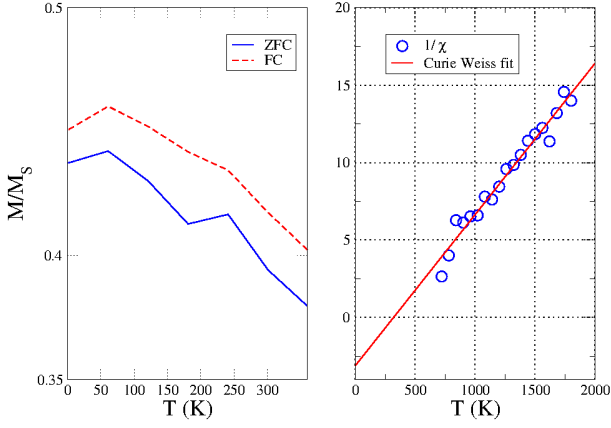


FIG. 6. (colour online) Left: ZFC-FC plots for the magnetization in the case of 25% antisite disorder in 2D. Right: Curie Weiss fit to the reciprocal susceptibility for the disordered case.

This is a consequence of the majority spin hybridization between B and B' site electrons in the hamiltonian of Eq 2 for LNMO, as opposed to minority spin hybridization as in SFMO¹⁸. This explains why LNMO is ferromagnetic, as opposed to SFMO, which is ferrimagnetic. This is also supported by the fact that the Nickel e_g up and down spin bands do not lie within the exchange gap of the Mn e_g bands (see DOS of Fig 3), as opposed to SFMO where the spin-split Mo orbitals lie within the exchange gap of Fe, inducing a moment in Mo opposite to Fe²¹. The magnetization (M) versus temperature in 2D plotted in left panel of Fig 5 shows a single transition with a T_c around 360K, while the Curie-Weiss fit of the inverse susceptibility gives a T_c around 250K. The M vs T plot in 3D is shown in the left panel of Fig 7. The T_c is similar (around 350K). The parameters used were: $t_{MN}=0.125$ eV, $\Delta=1.9$ eV, $J_{super}S=-7.5$ meV (2D) and -5 meV (3D)^{22,23}. The ordered moment reaches 90% of the maximum value at a temperature of about 1 K.

The effective exchange for an effective B-site (Mn) core spin-only model can be calculated from the Hamiltonian of Eq 2 by integrating out the B' (Ni) sites of the DP $\text{La}_2\text{NiMnO}_6$, using the procedure of Self-Consistent Renormalization (SCR)^{14,24}. As in Ref⁸, if we assume a onsite anisotropy on the Ni site then the J_{super} term in Eq 2 becomes diagonal. In the case of all spins lying parallel to this anisotropy axis ($\theta = 0$ or $\theta = \pi$), the effective exchange for a Mn core-spin-only model^{8,14}

$H = \sum J_{ij}^{eff} \sqrt{\frac{1+\vec{S}_i \cdot \vec{S}_j}{2}}$ can be evaluated as (considering majority spin hybridization with $J_H \rightarrow -\infty$ rather than minority spin hybridization with $J_H \rightarrow \infty$ as in Ref⁸):

$$J_{ij}^{eff} = \sum_k \frac{1}{2} [E_{k+} n_F(E_{k+}) + E_{k-} n_F(E_{k-}) - (\Delta - J'_{super}) n_F(\Delta - J'_{super})] e^{i\vec{k} \cdot (\vec{r}_i - \vec{r}_j)} \quad (8)$$

where $E_{k\pm} = \frac{(\Delta - J'_{super}) \pm \sqrt{(\Delta - J'_{super})^2 + 4\epsilon_k^2}}{2}$, $J'_{super} =$

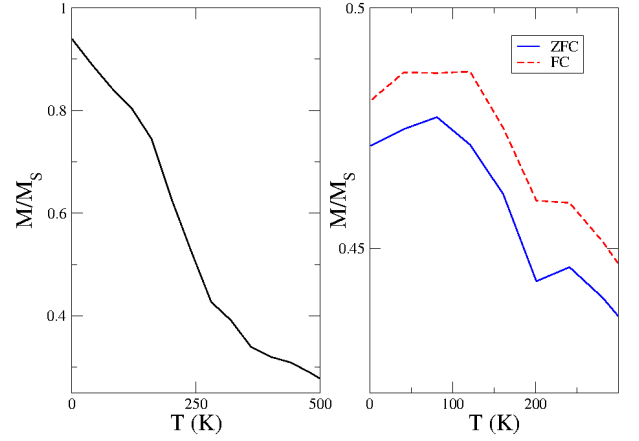


FIG. 7. (colour online) Left: Magnetization vs temperature plot in the ordered case in 3D. Right: ZFC-FC plots for magnetization vs temperature in the case of 25% antisite disorder in 3D.

$zJ_{super}S/2$. However, since the the Ni-Mn superexchange J_{super} is ferromagnetic, $J'_{super} < 0$, unlike the Cr-Os superexchange J_2 as defined in Ref⁸ which is antiferromagnetic, $J_2 > 0$. Hence the effective exchange expression becomes identical to that of Ref⁸ with $|J'_{super}|$ instead of $|J_2|$.

In LNMO, only the lowest band out of the 3 bands given in Eq 5 is occupied: this signifies the Nickel e_g majority spin band. Shifting the energies of the 3 bands by $-\frac{zJ_{super}S}{2}$, and putting $\tilde{\epsilon}_{Mn} = \epsilon_{Mn} + \frac{J_H S}{2} = \Delta$ and $\epsilon_{Ni} = 0$, the dispersions of the 3 shifted bands become:

$$\begin{aligned} \epsilon'_1 &= -zJ_{super}S \\ \epsilon'_\pm &= 0.5 \left[\left(\Delta - \frac{zJ_{super}S}{2} \right) \pm \sqrt{\left(\Delta - \frac{zJ_{super}S}{2} \right)^2 + 4\epsilon_k^2} \right] \end{aligned} \quad (9)$$

Hence there are 3 shifted bands centered at ≈ 0 , $-zJ_{super}S$ and $\left(\Delta - \frac{zJ_{super}S}{2} \right)$. Out of these, in LNMO, only the lowest Ni e_g band, signified by ϵ'_- , is occupied, as the electron filling is 1 per Ni e_g orbital (this is a single orbital model). Hence in the expression for effective exchange between Mn core t_{2g} classical core spins given by Eq 8, only the Fermi function for E_{k-} is non-zero at $T=0$. In the limit of small Ni-Mn hopping compared to Ni-Mn charge transfer energy and superexchange ($\frac{t_{MN}^2}{\Delta - J'_{super}} \rightarrow 0$), $E_{k-} \rightarrow \frac{1}{2} (\Delta - J'_{super}) \left[1 - \sqrt{1 + \frac{4\epsilon_k^2}{(\Delta - J'_{super})^2}} \right] \rightarrow \frac{1}{2} (\Delta - J'_{super}) \left[1 - \left\{ 1 + \frac{2\epsilon_k^2}{(\Delta - J'_{super})^2} \right\} \right] \rightarrow \frac{-\epsilon_k^2}{(\Delta - J'_{super})}$. Hence

$$J_{ij}^{eff} \rightarrow \frac{1}{2} \sum_k E_{k-} e^{i\vec{k} \cdot (\vec{r}_i - \vec{r}_j)}$$

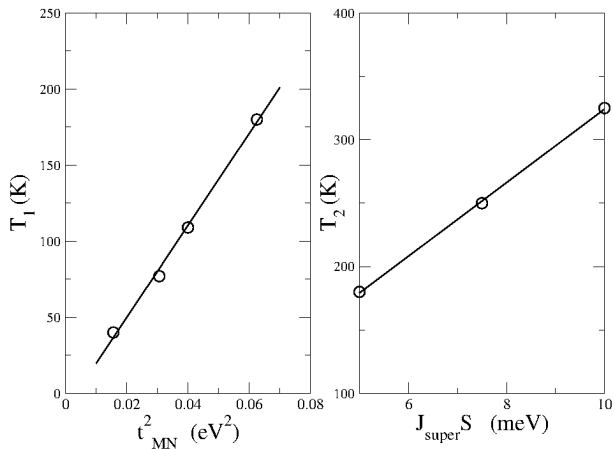


FIG. 8. Variation of the two temperatures of the kink anomalies in the magnetization with parameters, obtained from ED-MC simulations. Left: Variation of temperature T_1 of lower temperature anomaly with t_{MN}^2 , for constant J_{super} . Right: Variation of temperature T_2 of higher temperature anomaly with J_{super} , for constant t_{MN} .

$$\begin{aligned} &\rightarrow \sum_k \frac{-\epsilon_k^2}{2(\Delta - J'_{\text{super}})} e^{i\vec{k} \cdot (\vec{r}_i - \vec{r}_j)} \\ &\rightarrow \frac{-h_{ij}}{2(\Delta - J'_{\text{super}})} \end{aligned} \quad (10)$$

where $h_{ij} = t_{MN}^2 (\sum_{2\hat{x}} \delta_{i+2\hat{x},j} + 2 \sum_{\hat{x}+\hat{y}} \delta_{i+\hat{x}+\hat{y},j} + 4\delta_{ij})$ is the Fourier transform of ϵ_k^2 defined in Ref¹⁴. It involves a third neighbour term, a next-nearest neighbour term, and an onsite term. Hence the effective exchange between large B site classical core spins (Mn t_{2g} core spins) in LNMO, with a filling of one electron per Ni e_g orbital, is *ferromagnetic*, just like that (between Cr t_{2g} core spins) in SCO⁸, which has a filling of one electron per Os orbital. Thus the *core spin ferromagnetism* of LNMO arises from a similar interplay of double exchange J_H and superexchange J_{super} as in SCO, except that these are both ferromagnetic in the former, while both are antiferromagnetic in the latter. Thus when the B' sites are included, these two exchanges produce overall ferromagnetism in LNMO, and overall ferrimagnetism in SCO.

V. DISORDERED CASE: REENTRANT SPIN-GLASS TRANSITION

ED-MC simulations with $H = H_{\text{ord}}^{(1)} + H_{\text{disord}}$ for the case of 25% random antisite disorder were performed with a maximum system size of 16×16 in 2D, and $8 \times 8 \times 8$ in 3D. The results are shown in Fig 6, the right panel of Fig 7, and in Fig 8 and Fig 9. ZFC and FC plots for the magnetization are shown in the left panel of Fig 6 for 2D. Parameters chosen are similar to the ordered case²⁵. The 3D results for the ZFC and FC plots of the magnetization are shown in the right panel of Fig 7. The ZFC magnetization shows a kink at around 250K cor-

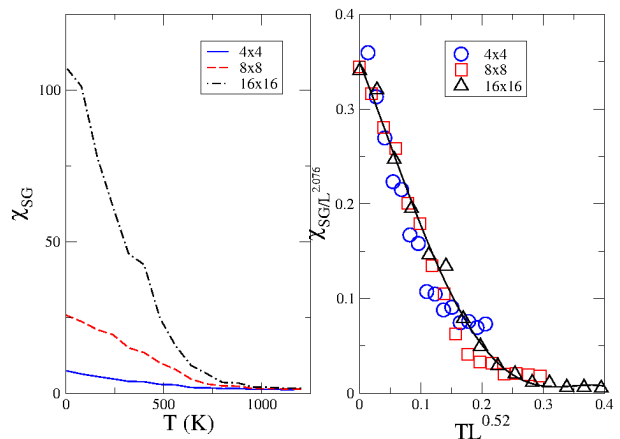


FIG. 9. (color online) Left: Spin-glass susceptibility vs temperature for the case of 25% antisite disorder in 2D. Right: Data collapse for finite size scaling with $T_{\text{SG}} < 0.01$, $\eta = -0.076$, $\nu = 1.92$ (T in eV)³².

responding to a transition to a disordered ferromagnetic state, followed by another kink at around 50K, signifying the onset of a new frustrated regime, where the system exhibits a tendency to become a spin-glass at low temperatures. This is similar to the signature of the reentrant spin-glass transition observed experimentally by D. Choudhury et.al.⁵. The ZFC-FC diverges throughout this temperature range, and the moment reaches only about 45-48% of its saturation value. The Curie Weiss fit to the high temperature susceptibility gives a T_c of about 320K while the low temperature kink anomaly in the magnetization starts around 150K, and the highest value of moment is reached around 50K, indicative of the frustration in the system²⁶.

In order to explore the systematics of the two kink anomalies in the magnetization vs temperature curve, ED-MC simulations were carried out for the 25% disordered systems with varying parameter sets (not just the parameter set obtained from DFT data of Ref⁶ quoted before). The results are shown in Fig 8. It is observed that the temperature T_1 for the low temperature anomaly varies as the square of the Mn-Ni hopping amplitude t_{MN} (left panel of Fig 8), when J_{super} is maintained constant. Whereas, the temperature T_2 at which the high temperature anomaly occurs varies proportional to J_{super} (right panel of Fig 8), when t_{MN} is maintained constant.

In order to confirm the spin-glass behaviour of this disordered system, the spin-glass susceptibility^{27,28} is plotted versus temperature in the left panel of Fig 9, in 2D for system sizes 4×4 , 8×8 and 16×16 respectively. It is found to diverge at low temperatures, confirming that the system is indeed a spin-glass. Finite size scaling has been undertaken in the right panel of Fig 9. Upon scaling the spin-glass susceptibility as $\frac{\chi_{\text{SG}}}{L^{2-\eta}}$ and plotting this versus $(T - T_{\text{SG}})L^{1/\nu}$ (where T is expressed in eV), the data for the 3 different system sizes are found to collapse to the same curve for the choice

$T_{SG} < 116K, \eta = -0.076, \nu = 1.92^{29-32}$. The scaling exponents η and ν are intermediate between those for the disordered 2D Ising model²⁸ and the disordered 3D classical Heisenberg model³¹.

As the ordering temperature for the high temperature ferromagnetic phase is $\approx 250-300K$, which is close to the T_c of the ferromagnetic phase in the ordered case, this ordering scale is clearly set by the Mn-Ni superexchange $zJ_{super}S$ ($\approx 300K$). The low temperature frustrated phase accompanied by a kink anomaly in the magnetization, is presumably due to the competition of the ferromagnetic Mn-Mn effective double exchange scale set by $\frac{t_{MN}^2}{2(\Delta - J_{super}')} (\approx 50K, \text{ from } J_{ij}^{eff} \text{ in Eq 10})$, with the antiferromagnetic antisite Mn-Mn superexchange J_{AS} . The presence of two ferromagnetic scales, namely due to Mn-Ni superexchange and effective Mn-Mn double exchange along with the antiferromagnetic antisite Mn-Mn superexchange J_{AS} in LNMO presumably leads to the reentrant spin-glass or reentrant ferromagnetic behaviour. Such a competition between double exchange and superexchange leading to reentrant spin-glass behaviour have also been observed in other materials³³. Thus, a rough estimate of the two temperatures related to the reentrant spin-glass transition, can be obtained as $T_2 \approx zJ_{super}S$ corresponding to a transition to a high temperature superexchange dominated regime and $T_1 \approx \frac{t_{MN}^2}{2(\Delta - J_{super}')}$, signifying the onset of a low temperature double exchange dominated regime³⁴. The observed dependence of the two kink anomalies in the magnetization upon parameters t_{MN} and J_{super} (namely $T_1 \propto t_{MN}^2$ and $T_2 \propto J_{super}$), obtained from ED-MC simulations (Fig 8) as discussed before, is consistent with this picture. This establishes that the observed kink anomalies in the magnetization are indeed signatures of a changeover from a superexchange dominated to a double exchange dominated regime.

It is to be noted that the two transitions as observed in the ZFC happen in a single homogeneous phase involving Ni^{2+} - Mn^{4+} ions and not two phases consisting of Ni^{2+} - Mn^{4+} and Ni^{3+} - Mn^{3+} respectively, as suggested in some previous works⁴. As is evident from Fig 4, the moment on the e_g orbitals resides almost entirely on the Nickel, and very little on the Manganese site. Thus, the Nickel maintains its Ni^{2+} character and the Manganese its Mn^{4+} character, as reported in Ref⁵. Thus our results support the idea of a reentrant spin-glass transition within a single homogeneous phase of disordered La_2NiMnO_6 , as proposed in Ref⁵.

VI. CONCLUSION

In conclusion, a plausible explanation for the ferromagnetic insulating ground state of ordered La_2NiMnO_6 along with the reentrant spin-glass behaviour observed in presence of antisite disorder, is provided in a unified framework. The importance of the Ni-Mn superexchange

in realizing the correlated ferro insulating state in the ordered case is established. Salient features of the DFT DOS are explained using this simple model Hamiltonian. The relevant energy scales which dictate the magnetism are identified. The underlying physics of the reentrant spin-glass transition is explained in terms of a changeover from a high temperature ferromagnetic superexchange dominated regime to a low temperature ferromagnetic double exchange dominated regime, in competition with the antiferromagnetic antisite superexchange. A novel mechanism of majority spin hybridization is proposed to explain the ferromagnetic behaviour of ordered LNMO as opposed to ferrimagnetic behaviour of many other DP-s like SFMO.

VII. APPENDIX: MAJORITY SPIN HYBRIDIZATION

Let us consider a two-sublattice Kondo lattice model suitable for double perovskites, of the form of Eq 1, for simplicity without the superexchange term.

$$H_{ord} = \epsilon_{Ni} \sum_{i\sigma} c_{N,i\sigma}^\dagger c_{N,i\sigma} + \epsilon_{Mn} \sum_{i\sigma} c_{M,i\sigma}^\dagger c_{M,i\sigma} + t_{MN} \sum_{\langle ij \rangle > \sigma} c_{M,i\sigma}^\dagger c_{N,j\sigma} + J \sum_{i\alpha,\beta} c_{M,i\alpha}^\dagger \vec{\sigma}_{\alpha\beta} c_{M,i\beta} \cdot \vec{S}_i \quad (11)$$

Then the Kondo coupling term $J \sum_{i\alpha,\beta} c_{M,i\alpha}^\dagger \vec{\sigma}_{\alpha\beta} c_{M,i\beta} \cdot \vec{S}_i$ can be diagonalized by using a transformation of the Fermion operators $c_{M,i\uparrow}$ and $c_{M,i\downarrow}$ as follows¹⁸:

$$c_{M,i\uparrow} = \cos \frac{\theta}{2} m_{iu} + \sin \frac{\theta}{2} m_{il} \\ c_{M,i\downarrow} = \sin \frac{\theta}{2} e^{i\phi} m_{iu} - \cos \frac{\theta}{2} e^{i\phi} m_{il} \quad (12)$$

For DP-s like Sr_2FeMoO_6 (SFMO), an antiferromagnetic Kondo coupling ($J > 0$) is considered^{7,18}, and hence in the limit $J \rightarrow \infty$, all terms involving m_{iu} operators are neglected. Then m_{il} is set equal to spinless operator m_i . The hybridization terms of such a $J \rightarrow \infty$ model (as in Ref¹⁸), written in the same notation convention as followed in this manuscript, is given by:

$$t_{MN} \sum_{\langle ij \rangle} \left(\sin \frac{\theta_i}{2} m_i^\dagger c_{N,j\uparrow} - e^{i\phi_i} \cos \frac{\theta_i}{2} m_i^\dagger c_{N,j\downarrow} \right) + h.c. \quad (13)$$

Obviously, if all the B site core spins \vec{S}_i point upwards, $\theta_i = 0, \phi_i = 0 \forall i$, whereupon the B-site spinless Fermions m_i hybridize only with the minority down spin B' site electrons $c_{N,j\downarrow}$. Thus *minority spin hybridization* is obtained, which leads to *ferrimagnetism* in DP-s like SFMO, with the B' site moment pointing opposite to the B site moment. This is because the minority B' site electrons form a band due to hybridization which is partially or wholly occupied, while the majority B' site electrons are localized, and hence remain above the Fermi energy.

On the other hand, the model for LNMO that is presented in Eq 1 considers a ferromagnetic Kondo coupling, which in this case is nothing but the Hund coupling $J = J_H$. Then in the limit $J \rightarrow -\infty$, the m_{il} terms are neglected, and m_{iu} are set equal to the spinless Fermion operator m_i . The resultant model as in Eq 2, has the following hybridization terms in the $J \rightarrow -\infty$ limit:

$$t_{MN} \sum_{\langle ij \rangle} \left(\cos \frac{\theta_i}{2} m_i^\dagger c_{N,j\uparrow} + \sin \frac{\theta_i}{2} e^{i\phi_i} m_i^\dagger c_{N,j\downarrow} \right) + h.c. \quad (14)$$

In this case, if all the B site core spins \vec{S}_i point upwards, i.e., $\theta_i = 0, \phi_i = 0 \forall i$ then the B site spinless fermions m_i hybridize only with the majority spin B' site electrons $c_{N,j\uparrow}$. Hence the majority spin B' site electrons form

a band which in this case is fully occupied, while the minority spin B' site electrons are mostly localized, and remain above the Fermi energy. Thus we get *majority spin hybridization* in the $J_H \rightarrow -\infty$ model given by Eq 2, leading to *ferromagnetism* in LNMO, with the B' moment pointing parallel to the B site moment.

ACKNOWLEDGMENTS

The author acknowledges useful discussions with D. Choudhuri, H. Das, T. Saha Dasgupta and D.D. Sarma, and financial support through FIG 100625, and also use of the Kalam HPC cluster (DST-FIST project), and UNAST cluster of SN Bose National Center for Basic Sciences.

-
- ¹ N. S. Rogado, J. Li, A. W. Sleight and M. A. Subramanian, Adv. Mater. **17**, 2225 (2005).
 - ² H. Guo, J. Burgess, S. Street, A. Gupta, G. Calvaresi and M. A. Subramanian, Appl. Phys. Lett. **89**, 022509 (2006).
 - ³ A. M. Cook and A. Paramakanti, Phys. Rev. Lett. **113**, 077203 (2014).
 - ⁴ R.I. Dass, J. Q. Yan and J.B. Goodenough, Phys. Rev. B **68**, 064415 (2003).
 - ⁵ D. Choudhuri, P. Mandal, R. Mathieu, A. Hazarika, S. Rajan, A. Sundaresan, U.V. Waghmare, R. Knut, O. Karis, P. Nordblad and D.D. Sarma, Phys. Rev. Lett. **108**, 127201 (2012).
 - ⁶ Hena Das, Umesh V. Waghmare, T. Saha-Dasgupta, and D.D. Sarma, Phys. Rev. Lett. **100**, 186402 (2008).
 - ⁷ A. Chattopadhyay and A.J. Millis, Phys. Rev. B **64**, 024424 (2001).
 - ⁸ Prabuddha Sanyal, Phys. Rev. B **89**, 115129 (2014).
 - ⁹ Sanjeev Kumar, Gianluca Giovannetti, Jeroen van den Brink and Silvia Picozzi, Phys. Rev. B **82**, 134429 (2010).
 - ¹⁰ In LNMO, the Manganese is in Mn^{4+} state and the Nickel in Ni^{2+} state according to Ref⁵ and Ref⁶. The electronic configuration of Ni^{2+} is $t_{2g}^2 e_g^2$, while that of Mn^{4+} is $t_{2g}^3 e_g^0$. Thus the Nickel e_g orbitals are half filled, while the Mn e_g orbitals are empty. The empty e_g orbitals of Mn^{4+} being Jahn-Teller inactive, the electron-phonon interaction is neglected. Again, since the Nickel e_g orbitals are half-filled, the orbital moment is expected to be nearly quenched. Thus, spin-orbit coupling is not found to affect the DFT results drastically⁶ and hence is neglected. For these reasons, a single e_g orbital model where the Nickel e_g orbital is half filled, and the Manganese e_g unfilled, suffices for the present study (See Fig 2).
 - ¹¹ O.N. Meetei, O. Erten, M. Randeria, N. Trivedi and P. Woodward, Phys. Rev. Lett. **110**, 087203 (2013).
 - ¹² K.I. Kugel and D.I. Khomskii, Sov. Phys. Usp. **25**, 231 (1982).
 - ¹³ Ref⁶ distinguishes between the Ni-Mn $e_g - e_g$ superexchange $J(1)$ which is FM and the Ni-Mn $e_g - t_{2g}$ superexchange $J(2)$ which is AFM and considers the net Ni-Mn superexchange J_{net} to arise as the additive effect of the two competing interactions ($J_{net} = J(1) + J(2)$). This net interaction J_{net} comes out to be FM and of magnitude $-5meV$. However, the Ni-Mn $e_g - e_g$ superexchange cannot be considered in the present work as then the Hamiltonian ceases to have spin-Fermion interactions which are coupled classical-quantum interactions, and instead would have four-Fermion fully quantum mechanical interactions which can no longer be treated by the ED-MC method. The Ni-Mn $e_g - t_{2g}$ superexchange can however, be treated using this method as that is between classical t_{2g} core spins and quantum Ni e_g Fermions. Hence this Ni-Mn $t_{2g} - e_g$ superexchange is used as J_{super} in the model of Eq 1 but instead considered as FM, and the value of the net superexchange $J_{super}S = J_{net} = -5meV$ is used. While this is an approximation, it does not alter the physics greatly, as this J_{super} is taken as the only Ni-Mn superexchange, and hence the value as well as the sign of the net Ni-Mn superexchange as in the DFT paper of Ref⁶ is preserved.
 - ¹⁴ Prabuddha Sanyal and Pinaki Majumdar, Phys. Rev. B **80**, 054411 (2009).
 - ¹⁵ The $|J_H| \rightarrow \infty$ limit of double exchange models was introduced by Anderson and Hasegawa¹⁶ and later studied by P.De Gennes¹⁷ in the context of perovskites. This limit was studied in the context of double perovskites in Ref¹⁸, but they considered *antiferromagnetic* coupling ($J_H > 0, J_H \rightarrow \infty$), and obtained *minority spin hybridization*. In the present work *ferromagnetic* coupling ($J_H < 0$) $J_H \rightarrow -\infty$ limit is studied, and *majority spin hybridization* is obtained (See Appendix).
 - ¹⁶ P.W. Anderson and H. Hasegawa, Phys. Rev. **100**, 675 (1955).
 - ¹⁷ P. -G de Gennes, Phys. Rev. **118**, 141 (1960).
 - ¹⁸ J.L.Alonso, L.A. Fernandez, F. Guinea, F. Lesmes, and V. Martin-Mayor, Phys. Rev. B **67**, 214423 (2003).
 - ¹⁹ D.D. Sarma, Sugata Ray, K. Tanaka, M. Kobayashi, A. Fujimori, P. Sanyal, H.R. Krishnamurthy and C. Dasgupta, Phys. Rev. Lett. **98**, 157205 (2007).
 - ²⁰ The bandwidths are not accurately reproduced as a single-orbital model has been considered instead of the two e_g orbitals, and inter-orbital hopping has been neglected.
 - ²¹ D.D. Sarma, P. Mahadevan, T. Saha-Dasgupta, S. Ray and A. Kumar, Phys. Rev. Lett. **85**, 2549 (2000).

- ²² $J_{super}S$ in 3D is 2/3 of $J_{super}S$ in 2D, so that $zJ_{super}S$ remains constant at the value given in Ref⁶, where z is the coordination number.
- ²³ While the value of $J_{super}S = -5meV$ as in Ref⁶ correctly reproduces the ferromagnetic T_c , larger values are required to match the separation between the Nickel majority and minority e_g bands in the DFT DOS. The onsite Coulomb U on the Nickel e_g orbitals, neglected in this work, might have a role to play here.
- ²⁴ S. Kumar and P. Majumdar, Phys. Rev. Lett. **91**, 246602 (2003).
- ²⁵ The parameters used for the antisite disordered part are $t_{MN} = t_{MM} = t_{NN} = 0.125$, $J_{AS} = 0.025$, $h = 0.01$. The value of J_{AS} used in this work is intermediate between the values of nearest neighbour Heisenberg Mn t_{2g} core spin superexchange in rare-earth manganites (0.017 eV) as given in Ref³⁵, and the value of Fe-Fe antisite superexchange for the double perovskite Sr_2FeMoO_6 (0.035 eV) considered in Ref¹⁸.
- ²⁶ The next-nearest-neighbour B'-B' (Ni-Ni) superexchange which introduces an additional source of frustration even in the ordered case, like the Os-Os superexchange in SCO^{11} , has not been considered in this work.
- ²⁷ K.H.Fischer and J.A. Hertz, *Spin Glasses*, (Cambridge University Press, 1991).
- ²⁸ R.N. Bhatt and A.P. Young, Phys. Rev. B **37**, 5606 (1988).
- ²⁹ Yu. V. KopaeV, W. Hanke, *Electronic Phase Transitions Volume 32*, (Elsevier, 1992).
- ³⁰ H. Kawamura, Phys. Rev. Lett. **68**, 3785 (1992).
- ³¹ L.A. Fernandez, V. Martin-Mayor, S. Perez-Gavero, A. Tarancon and A.P.Young, Phys. Rev. B **80**, 024422 (2009).
- ³² Since the temperature scale in the data collapse plot is in eV, the error in determining T_{SG} is about 0.01 eV for 2D. Hence the only definitive statement that can be made about T_{SG} is that it is less than 116K in 2D.
- ³³ R. Mathieu, P. Svedlindh, and P. Nordblad, Europhys. Lett. **52**, 441 (2000).
- ³⁴ While this temperature T_1 signifies the onset of a frustrated double exchange dominated regime, when the effective Mn-Mn double exchange begins to compete with the antisite Mn-Mn superexchange, and spin-glass correlations begin to proliferate, the actual spin-glass transition T_{SG} may occur at lower temperatures.
- ³⁵ E. Dagotto, T. Hotta and A. Moreo, Phys. Rep. **344**, 1 (2001).